Roles of Surface Hydrophobic Residues in the Interfacial Catalysis of Bovine Pancreatic Phospholipase A_2[†]

Byung-In Lee, Edward T. Yoon, and Wonhwa Cho*

Department of Chemistry (M/C 111), University of Illinois at Chicago, 845 West Taylor Street, Chicago, Illinois 60607-7061

Received October 17, 1995; Revised Manuscript Received January 4, 1996[⊗]

ABSTRACT: The interfacial binding is a unique and important step in the phospholipase A_2 (PLA_2) catalyzed hydrolysis of phospholipids which is distinct from the binding of a substrate to the active site. To assess the roles of surface hydrophobic residues of PLA_2 in these processes, we selectively mutated Leu-19 and Leu-20 of bovine pancreatic PLA_2 to charged (L19K and L20K), uncharged polar (L19S and L20S), and amphiphilic (L19W and L20W) groups and measured their kinetic and binding properties using various phospholipid aggregates, including micelles, monolayers, and polymerized mixed liposomes. The mutations of Leu-19 and Leu-20 did not significantly change either the tertiary structure or the thermodynamic stability of bovine pancreatic PLA_2. Toward monomeric 1,2-dihexanoyl-*sn*-glycero-3-phosphocholine, all Leu-20 mutants (L20S, L20W, and L20K) showed activities comparable to that of wild type whereas the substitution of Leu-19 with less hydrophobic side chains (L19S and L19K) reduced the activity to 70% and 50%. Toward zwitterionic 1,2-dioctanoyl-*sn*-glycero-3-phosphocholine (diC_8PC) micelles, L20S and L20K mutants showed only 30% and 35% of the wild-type activity, respectively, whereas L20W was about twice as active as wild type. Also, L19S and L19K showed 75% and 15% of the wild-type activity, respectively. Toward anionic Triton X-100/sodium deoxycholate/diC_8PC (4:2:1) mixed micelles, L20W and L20K were 2.6 times and twice more active than wild type. To determine the *sn*-2 acyl group selectivity of wild type and mutants, polymerized mixed liposomes were used which contained 1,2-bis[12-(lipoyloxy)-dodecanoyl]-*sn*-glycero-3-phosphoglycerol and 1 mol % of either 1-[12-(1-pyrenebutanoyloxy)dodecanoyl]-2-hexanoyl-*sn*-glycero-3-phosphocholine or 1-[12-(1-pyrenebutanoyloxy)dodecanoyl]-2-dodecanoyl-*sn*-glycero-3-phosphocholine. These measurements showed that Leu-19 was involved in the substrate binding and the *sn*-2 acyl group selectivity of bovine pancreatic PLA_2 and that Leu-20 made a direct contact with the surface of phospholipid aggregates. The binding affinities of mutants to micelles, polymerized liposomes, and monolayers were well consistent with their kinetic behaviors, supporting the notion that the altered activities of Leu-19 mutants and Leu-20 mutants were due to the change in their substrate binding and interfacial binding, respectively. Finally, the L20W mutant represents the first example of protein engineering of PLA_2 which results in a significant increase in interfacial binding to densely packed neutral monolayers and bilayers.

Phospholipase A_2 (PLA_2;[1] EC 3.1.1.4) catalyzes the hydrolysis of the fatty acid ester in the 2-position of 3-*sn*-phospholipids [for recent reviews, see Dennis (1994), Gelb et al. (1995), and Scott and Sigler (1994)]. Because PLA_2 acts at the lipid−water interface, the PLA_2 catalysis involves the binding of protein to the interface. This interfacial binding is a unique and important step in the interfacial catalysis of PLA_2 and generally occurs prior to the binding of a substrate to the active site (Jain & Berg, 1989). Extensive structural (Dijkstra et al., 1981a; Scott et al., 1990) and mutational studies (Dua et al., 1995; Kuipers et al., 1990; Liu et al., 1995) on several secretory PLA_2s have indicated that PLA_2 has an interfacial binding site topologically distinct from the active site. The putative interfacial binding site of secretory PLA_2 is located on a flat molecular surface which contains several hydrophobic residues forming a rim of the hydrophobic channel (see Figure 1) and ionic residues surrounding these hydrophobic residues. Surface cationic residues have been implicated in diverse pharmacological activities of secretory PLA_2s, such as anticoagulant activity (Kini & Evans, 1987). Recently, we have performed a structure-function study on bovine pancreatic PLA_2 by the site-specific mutagenesis and the kinetic analysis using a newly developed polymerized mixed liposome system and shown that some cationic residues in the interfacial binding surface play a critical role in its binding to anionic interfaces (Dua et al., 1995). The primary objective of this study is to understand the roles of hydrophobic residues (e.g., Leu-2, Trp-3, Leu-19, Leu-20, Leu-31, Tyr-69; see Figure 1) forming the rim of the hydrophobic channel of bovine

[†] This work was supported by an Arthritis Investigator Award and a Biomedical Science Grant from the Arthritis Foundation and a Grant-in-Aid from the American Heart Association (AHA 92-700).

* To whom correspondence should be addressed: telephone, 312-996-4883; Fax, 312-996-0431; email, wcho@uic.edu.

[⊗] Abstract published in *Advance ACS Abstracts,* March 1, 1996.

[1] Abbreviations: BLPC, 1,2-bis[12-(lipoyloxy)dodecanoyl]-*sn*-glycero-3-phosphocholine; BLPG, 1,2-bis[12-(lipoyloxy)dodecanoyl]-*sn*-glycero-3-phosphoglycerol; BSA, bovine serum albumin; CD, circular dichroism; diC_6PC, 1,2-dihexanoyl-*sn*-glycero-3-phosphocholine; D-diC_6-PC, 2,3-dihexanoyl-*sn*-glycero-1-phosphocholine; diC_8PC, 1,2-dioctanoyl-*sn*-glycero-3-phosphocholine; PC, phosphatidylcholine; PLA_2, phospholipase A_2; pyr-C_6PC, 1-[12-(1-pyrenebutanoyloxy)dodecanoyl]-2-hexanoyl-*sn*-glycero-3-phosphocholine; pyr-$C_{12}PC$, 1-[12-(1-pyrenebutanoyloxy)dodecanoyl]-2-dodecanoyl-*sn*-glycero-3-phosphocholine; pyrene-PC, 1-hexadecanoyl-2-(1-pyrenedecanoyl)-*sn*-glycero-3-phosphocholine; pyrene-PG, 1-hexadecanoyl-2-(1-pyrenedecanoyl)-*sn*-glycero-3-phosphoglycerol; D-POPC, 2-oleoyl-3-palmitoyl-*sn*-glycero-1-phosphocholine; SDS, sodium dodecyl sulfate.

0006-2960/96/0435-4231$12.00/0

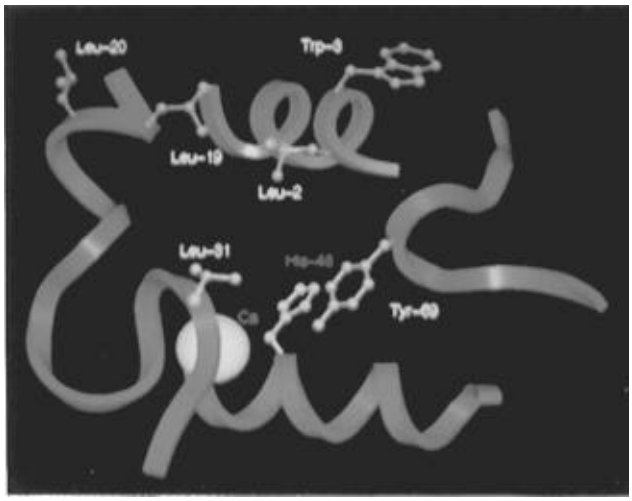

FIGURE 1: Partial ribbon diagram of bovine pancreatic PLA_2 illustrating several hydrophobic side chains forming a rim of hydrophobic channel (Dijkstra et al., 1981b). The calcium ion and His-48 in the active site are highlighted in yellow.

pancreatic PLA_2. Recent mutagenesis studies on bovine and porcine pancreatic PLA_2s (Kuipers et al., 1989, 1990; Liu et al., 1995) indicated that Trp-3 is involved in interfacial binding whereas Leu-2, Leu-31, and Tyr-69 are involved in substrate binding. In this study, we selectively mutated Leu-19 and Leu-20 of bovine pancreatic PLA_2 to charged (Lys), uncharged polar (Ser), and amphiphilic aromatic (Trp) side chains to understand roles of these surface hydrophobic residues in interfacial binding and substrate binding of bovine pancreatic PLA_2. Another impetus of this mutagenesis study is to convert bovine pancreatic PLA_2, which normally shows extremely low activity toward densely packed neutral phospholipid bilayers, into a neutral-bilayer-active form, based on the finding that many snake venom PLA_2s (e.g., *Naja naja naja* PLA_2) with high activity toward densely packed bilayers contain Trp residues at these positions. Herein, we present kinetic and binding properties of mutant proteins toward various types of substrates, including monomer, micelles, monolayers, and polymerized mixed liposomes. The results demonstrate the distinct roles of these hydrophobic residues in the interfacial catalysis of bovine pancreatic PLA_2 and provide insights into how Trp residues in the interfacial binding site enhance the enzyme activity toward densely packed neutral phospholipid monolayer and bilayers.

MATERIALS AND METHODS

1,2-Dihexanoyl-*sn*-glycero-3-phosphocholine (diC_6PC) and 1,2-dioctanoyl-*sn*-glycero-3-phosphocholine (diC_8PC) were purchased from Avanti Polar Lipids. 1-Hexadecanoyl-2-(1-pyrenedecanoyl)-*sn*-glycero-3-phosphocholine (pyrene-PC) and -phosphoglycerol (pyrene-PG) were obtained from Molecular Probes. D-α-glycerophosphocholine was a generous gift from Dr. Charles Pidgeon of Purdue University. Large unilamellar liposomes of BLPG (or mixed liposomes) were prepared by multiple extrusion of the phospholipid dispersion in 10 mM Tris-HCl buffer (pH 8.4) through a 0.1-μm polycarbonate filter (Millipore) in a microextruder Liposofast (Avestin, Ottawa, Ontario) and then polymerized in the presence of 10 mM dithiothreitol as described (Wu & Cho, 1994). Phospholipid concentrations were determined by phosphate analysis (Kates, 1986). The mean hydrodynamic radius of liposomes was determined by dynamic light scattering measurement as described (Budzynski et al., 1992). Fatty acid-free bovine serum albumin (BSA) was from Miles Inc. Guanidinium chloride was from Fisher. All the restriction enzymes, T4 ligase, and T4 polynucleotide kinase were obtained from Boehringer Mannheim Biochemicals. Oligonucleotides were purchased from Midland Co (Midland, TX).

Synthesis of Phospholipid. 2-Oleoyl-3-palmitoyl-*sn*-glycero-1-phosphocholine (D-POPC) was synthesized from 1-palmitoyl-*rac*-glycero-3-phosphocholine (Sigma) as previously described (Shen et al., 1994). 2,3-Dihexanoyl-*sn*-glycero-1-phosphocholine (D-diC_6PC) was synthesized by the esterification of D-α-glycerophosphocholine with hexanoic acid. 1,2-bis[12-(lipoyloxy)dodecanoyl]-*sn*-glycero-3-phosphocholine (BLPC) and -glycerol (BLPG) were synthesized as described previously (Wu & Cho, 1993). 1-[12-(1-Pyrenebutanoyloxy)dodecanoyl]-2-hexanoyl-*sn*-glycero-3-phosphocholine (pyr-C_6PC) and 1-[12-(1-pyrenebutanoyloxy)dodecanoyl]-2-dodecanoyl-*sn*-glycero-3-phosphocholine (pyr-C_{12}PC) were synthesized as follows. First, 1,2-bis[12-(1-pyrenebutanoyloxy)dodecanoyl]-*sn*-glycero-3-phosphocholine was synthesized from L-α-glycerophosphocholine (Sigma), 12-hydroxydodecanoic acid (Aldrich), and 1-pyrenebutanoic acid (Aldrich) as described for the synthesis of BLPC (Wu & Cho, 1993). After its hydrolysis by *Agkistrodon piscivorus piscivorus* venom (Shen et al., 1994), the esterification of chromatographically purified 1-[12-(1-pyrenebutanoyloxy)dodecanoyl]-2-hydroxy-*sn*-glycero-3-phosphocholine with hexanoic acid and dodecanoic acid yielded pyr-C_6PC and pyr-$C_{12}PC$, respectively.

Construction of Mutant Phospholipase A_2 Genes. The site-directed mutagenesis of bovine pancreatic PLA_2 was performed using the M13mp18 vector containing the bovine PLA_2 gene (Dua et al., 1995) according to the method of Nakamaye and Eckstein (1986) using an *in vitro* mutagenesis kit from Amersham. The oligonucleotides used for the construction of mutants were 5′ AAA ATC AAG CCA AGG CTC AGA 3′ (L19W), 5′ GTT AAA ATC CCA AAG AGG CTC 3′ (L20W), 5′ AAA ATC AAG AGA AGG CTC AGA 3′ (L19S), 5′ GTT AAA ATC AGA AAG AGG CTC 3′ (L20S), 5′ AAA ATC AAG TTT AGG CTC AGA 3′ (L19K), and 5′ ATT GTT AAA ATC TTT AAG AGG CTC AGA 3′ (L20K), respectively, in which underlined bases indicate the location of mutation. After DNA sequences of mutants were verified by the sequencing analysis (Sanger et al., 1977) using a Sequenase 2.0 kit (U.S. Biochemicals), individual recombinant PLA_2 genes were digested with *Eco*R1 and *Bam*H1 and inserted into the pTO-propla2 vector (Deng et al., 1990).

Protein Expression and Purification. Wild-type and mutant proteins were expressed in *Escherichia Coli* strain BL21(DE3)pLysS (Novagen) using the pTO-propla2 vector and purified as described (Dua et al., 1995). Purity of protein was confirmed by SDS−polyacrylamide electrophoresis and isoelectric focusing using a Phast system (Pharmacia). Protein concentrations were determined by the Micro bicinchoninic acid method (Smith et al., 1985) (Pierce). Circular dichroism (CD) spectra of proteins were measured in 10 mM phosphate buffer, pH 7.4, at 25 °C using a Jasco J-600 spectropolarimeter. Each spectrum was obtained at wavelengths between 195 and 300 nm from ten scans.

Measurements of Protein Stability. The stability of wild-type and mutant proteins was measured from the equilibrium denaturation by guanidinium chloride. Briefly, proteins were incubated in 10 mM phosphate buffer, pH 7.4, containing 0−8 M guanidinium chloride for 2 h at 25 °C and their CD spectra measured. Assuming a two-state protein folding (e.g., native ↔ unfolded), molar ellipticity values at 222 nm (θ_{222}) at different guanidinium chloride concentrations were converted to the fraction of unfolded protein (f_u) using an equation $f_u = (\theta_N - \theta_{222})/(\theta_N - \theta_U)$, where θ_N and θ_U indicate extrapolated baselines for the native and unfolded proteins, respectively (Pace, 1986; Santoro & Bolen, 1988). Free energy of folding ($\Delta G°_{fold}$) was determined from the nonlinear least-squares analysis of the f_u vs [guanidinium chloride] plot using an equation $f_u = 1/(1 + \exp[-(\Delta G°_{fold}/RT + m[\text{guanidinium chloride}]/RT)])$, where m indicates the slope of the plot in the transition region (Pace, 1986; Santoro & Bolen, 1988).

Kinetic Measurements. All the kinetic experiments were performed at 37 °C and at pH 7.4. PLA_2-catalyzed hydrolysis of polymerized mixed liposomes was carried out in 2 mL of 10 mM HEPES buffer, pH 7.4, containing 0.1 μM pyrene-containing phospholipid inserted in 9.9 μM BLPG, 2 μM BSA, 0.16 M NaCl, and 10 mM $CaCl_2$. The progress of hydrolysis was monitored as an increase in fluorescence emission at 378 nm using a Hitachi F4500 fluorescence spectrometer with the excitation wavelength set at 345 nm. Spectral bandwidth was set at 5 nm for both excitation and emission. The kinetic analysis of PLA_2-catalyzed hydrolysis of polymerized mixed liposomes was described in detail previously (Dua et al., 1995; Wu & Cho, 1993, 1994). In brief, an apparent specificity constant, $(k_{cat}/K_m)_{app}$, was calculated by dividing by enzyme concentration the pseudo-first-order rate constant which was calculated from the nonlinear least-squares analysis of reaction progress curves. Kinetics of PLA_2-catalyzed hydrolysis of diC_6PC monomers were performed with 0.5 mM phospholipid, 0.16 M NaCl, and 10 mM $CaCl_2$. The hydrolysis of diC_8PC micelles was measured in the presence of 0.5 mM diC_8PC, 0.16 M NaCl, and 10 mM $CaCl_2$. The hydrolysis of mixed micelles was measured in the presence of 2 mM Triton X-100, 1 mM sodium deoxycholate, 0.5 mM diC_8PC, 0.16 M NaCl, and 10 mM $CaCl_2$ as described previously (Dua & Cho, 1994). Time courses of the hydrolysis of phospholipids were monitored with a computer-controlled Metrom pH stat (Brinkmann) in a thermostated vessel. Under these conditions, the hydrolysis of both diC_6PC and diC_8PC followed the first-order kinetics because substrate concentrations were lower than apparent K_m values. Thus, $(k_{cat}/K_m)_{app}$ values were calculated by dividing by enzyme concentration the pseudo-first-order rate constants determined from the nonlinear least-squares analysis of reaction progress curves.

Binding Measurements. The binding of bovine PLA_2 and its mutants to polymerized liposomes was measured by two independent methods: fluorometry and centrifugation of sucrose-loaded polymerized liposomes. The former method was described in detail previously (Dua et al., 1995; Wu & Cho, 1993, 1994). The requirement of relatively high enzyme concentration (ca. 2 μM) for this fluorometric determination made it difficult to accurately determine the dissociation constants for the mutants, e.g., L20W, with enhanced interfacial binding affinity. To circumvent this difficulty, we employed a centrifugation method, based on the method of Rebecchi et al. (1992), which utilizes sucrose-loaded BLPG-polymerized liposomes and allows the use of lower enzyme concentrations (ca. 50 nM). Sucrose-loaded BLPG-liposomes were prepared in 10 mM Tris-HCl buffer, pH 8.4, containing 0.32 M sucrose, and polymerized for 30 h at 37 °C in the presence of 10 mM dithiothreitol. Non-entrapped sucrose molecules were removed by gel filtration chromatography using a Sephadex G-25 column equilibrated and eluted with 10 mM HEPES buffer, pH 7.4, containing 0.16 M NaCl. For the binding measurements, 0.1−50 μM BLPG polymerized liposomes were incubated with 50 nM protein solution in 10 mM HEPES buffer, pH 7.4, containing 0.145 M NaCl and 10 mM $CaCl_2$ for 30 min at room temperature. The mixtures (200 μL each) were then centrifuged at 100000*g* at room temperature using a Beckmann Airfuge ultracentrifuge with an A100 rotor to precipitate polymerized liposomes. As a control, sucrose-loaded BLPG-polymerized liposomes containing 0.1 mol % of tritiated 1-palmitoyl-2-oleoyl-*sn*-glycero-3-phosphocholine (Amersham) were prepared and 0.1−50 μM quantities of these liposomes were centrifuged under the same condition. The measurement of the residual radioactivity of supernatant showed that less than 2% of liposomes remained in solution after centrifugation. After centrifugation, the PLA_2 activity of each supernatant was assessed by measuring the initial velocity of the hydrolysis of pyrene-PC/BLPG-polymerized mixed liposomes as described (Wu & Cho, 1994). Then, the fractional saturation of PLA_2 (f = [bound PLA_2]/[total PLA_2]), calculated as a ratio of initial velocity determined for the mixture containing a given BLPG concentration to the initial velocity for the same mixture minus BLPG, was plotted as a function of total BLPG concentration ($[PL]_0$). Assuming each phospholipid molecule as a ligand that binds independently with apparent dissociation constant K_d to n equivalent sites on a PLA_2 molecule, values of both n and K_d were determined by the nonlinear least-squares analysis of the f vs $[PL]_0$ data using eq 1:

$$f = \{[E]_0 + K_d + [PL]_0/n - ([E]_0 + K_d + [PL]_0/n)^2 - 4[E]_0[PL]_0/n]^{1/2} \quad (1)$$

where $[E]_0$ represents total enzyme concentration. The binding of PLA_2 to the D-diC_6PC monomer was measured spectrophotometrically as described previously (Pieterson et al., 1974). Typically, to a 30 μM protein solution in 10 mM HEPES buffer, pH 7.4, containing 0.16 M NaCl and 10 mM $CaCl_2$ was added 0.1−10 mM D-diC_6PC. The increase in absorbance at 289 nm (ΔA) was measured at each D-diC_6-PC concentration using the same solution minus protein as a reference. The K_d value for each protein was determined from the nonlinear least-squares analysis of the binding isotherm using a simple Langmuir equation: $\Delta A/\Delta A_{max} = 1/(1 + K_d/[PL]_0)$, where ΔA_{max} and $[PL]_0$ indicate the maximal value of ΔA and total D-diC_6PC concentration, respectively.

Monolayer Measurements. Surface pressure (π) of solution in a circular Teflon trough was measured using a du Nouy ring attached to a computer-controlled Cahn electrobalance (Model C-32) and a small trough (5 cm diameter × 1 cm depth) as described previously (Mukhopadhyay & Cho, 1995; Shen & Cho, 1995; Shen et al., 1994). A total of 2−20 μL of phospholipid solution in ethanol/hexane (1:9

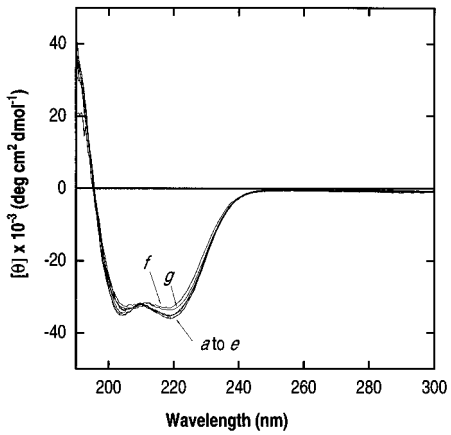

FIGURE 2: Circular dichroism spectra of bovine pancreatic PLA_2 (a) and its mutants including L19S (b), L20S (c), L19K (d), L20K (e), L19W (f), and L20W (g). Enzyme concentrations were 20 μM in 0.1 M phosphate buffer, pH 7.4.

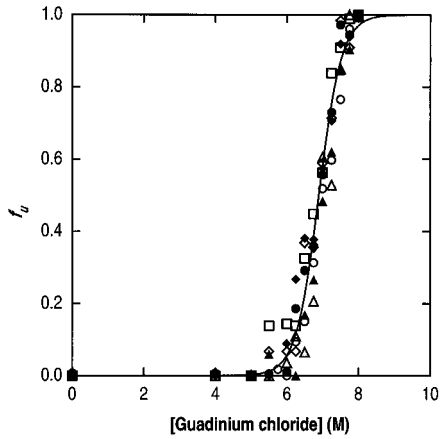

FIGURE 3: Guanidinium chloride-induced unfolding of bovine pancreatic PLA_2 (○) and its mutants including L19W (△), L20W (□), L19K (●), L20K (▲), L19S (◇), and L20S (◆) at 25 °C. Protein concentrations were 10 μM in 0.1 M phosphate buffer, pH 7.4. f_u values were calculated from θ_{222} values as described under Materials and Methods. A theoretical curve is shown for wild type which was constructed using its $\Delta G°_{fold}$ (=−12.5 kcal/mol) and m (=1.8 kcal mol^{-1} M^{-1}) values determined from the nonlinear least-squares analysis of data.

(v/v)) was spread onto the subphase containing 10 mM HEPES, pH 7.4, with 0.16 M NaCl and 10 mM $CaCl_2$ to form a monolayer with a given initial surface pressure (π_0). Once the surface pressure reading of the monolayer became stable (after 5−10 min), the protein solution was added to the subphase and the change in surface pressure ($\Delta\pi$) was measured as a function of time at 23 °C. Typically, the $\Delta\pi$ value reached a maximum after 5 min. The maximal $\Delta\pi$ value depended on the protein concentration at the low concentration range and reached a saturation when the protein concentration was higher than 0.1 μM. Protein concentrations were therefore maintained above 0.1 μM to ensure that the observed $\Delta\pi$ represented a maximal value and that a loss of protein by the adsorption to the trough wall was negligible.

RESULTS

Physical Properties of Mutants. Because the side chains of Leu-19 and Leu-20 of bovine pancreatic enzyme are largely exposed to solvent (see Figure 1), their mutations were not expected to have significant effects on the protein structure and stability. Indeed, all mutant proteins were expressed and refolded as efficiently as wild type (data not shown). Bovine pancreatic PLA_2 has a high α-helical content (Dijkstra et al., 1981b), as demonstrated by its characteristic CD spectrum. As shown in Figure 2, all mutants displayed similar CD spectra, and the estimations of the α-helical content from their θ_{222} values yielded similar results (ca. 50%). The CD data clearly show that mutations did not cause any gross structural change of protein. Minor differences in spectra for L19W and L20W might be due to the tendency of aromatic side chains to give rise to positive CD bands in the 215−230 nm range (Woody, 1994). Thermodynamic stability of wild type and mutants was determined from their guanidinium chloride-induced denaturation curves. As shown in Figure 3, the mutations did not show any significant effect on the stability of bovine pancreatic PLA_2. As summarized in Table 1, the curve fitting of unfolding data yielded similar values of $\Delta G°_{fold}$ and m for wild type and mutants within the range of experimental error and curve fitting. Taken together, these results indicate that the mutations did not significantly change either the tertiary structure or the thermodynamic stability of bovine pancreatic PLA_2.

Table 1: Free Energy of Folding[a] Determined from the Guanidinium Chloride-Induced Denaturation of Bovine Pancreatic PLA_2 and Its Mutants

enzyme	$-\Delta G°_{fold}$ (kcal/mol)	m (kcal mol^{-1} M^{-1})
wild type	12.5 ± 2.0	1.8 ± 0.2
L19W	13.5 ± 2.1	1.7 ± 0.3
L20W	11.5 ± 2.0	1.7 ± 0.3
L19S	12.2 ± 1.7	1.8 ± 0.4
L20S	10.7 ± 2.1	1.6 ± 0.2
L19K	12.5 ± 2.1	1.8 ± 0.3
L20K	13.5 ± 1.6	1.9 ± 0.2

[a]See Materials and Methods for experimental conditions and methods to calculate parameters. Values of m and $\Delta G°_{fold}$ represent best values ± standard deviations determined from the nonlinear least-squares analysis.

Kinetic Properties of Mutants toward Monomers and Micelles. To determine how differently the mutations of Leu-19 and Leu-20 affect the interfacial catalysis of bovine pancreatic PLA_2, we measured the activity of wild type and mutants toward phospholipid substrates in different physical states and with different surface charges: diC_6PC monomer, diC_8PC micelles, and diC_8PC in anionic mixed micelles of Triton X-100/sodium deoxycholate/diC_8PC (4:2:1) and pyrene-containing phosphatidylcholine (PC) in polymerized mixed liposomes. It has been well documented (Jain & Berg, 1989) that the interfacial catalysis of PLA_2 is sensitive to the interfacial properties of substrates, interfacial packing density, and surface charge in particular. For instance, it has been shown that both the interfacial binding site and active site of bovine pancreatic PLA_2 strongly prefer anionic phospholipids to neutral ones (Dua et al., 1995). To unambiguously sort out the effects of mutations on interfacial binding and substrate binding of PLA_2, we exclusively used PC as a hydrolyzable phospholipid interacting with the active site while varying interfacial properties of aggregates they form or they are embedded in. $(k_{cat}/K_m)_{app}$ values for wild-type and mutant proteins determined using various substrates are summarized in Table 2. Because PLA_2s do not follow conventional Michaelis−Menten kinetics in their hydrolysis of aggregated substrates, individual rate constants, k_{cat} and

Table 2: Kinetic Parameters[a] of Bovine Pancreatic PLA_2 and Its Mutants Determined Using Various Substrates

enzyme	monomeric diC_6PC $(k_{cat}/K_m)_{app} \times 10^3$ (M^{-1} s^{-1})	micellar diC_8PC $(k_{cat}/K_m)_{app} \times 10^5$ (M^{-1} s^{-1})	Tx-100/DC/diC_8PC[b] $(k_{cat}/K_m)_{app} \times 10^5$ (M^{-1} s^{-1})	pyr-C_6PC/BLPG[c] $(k_{cat}/K_m)_{app} \times 10^3$ (M^{-1} s^{-1})	pyr-C_{12}PC/BLPG[c] $(k_{cat}/K_m)_{app} \times 10^3$ (M^{-1} s^{-1})
wild type	1.0 ± 0.2	2.0 ± 0.2	1.6 ± 0.2	2.3 ± 0.3	11.5 ± 1.5
L19W	1.3 ± 0.2	2.3 ± 0.3	1.8 ± 0.3	2.5 ± 0.2	19.5 ± 1.5
L20W	1.2 ± 0.2	3.8 ± 0.3	4.2 ± 0.4	13.5 ± 1.5	66.0 ± 5.5
L19S	0.7 ± 0.1	1.5 ± 0.2	1.0 ± 0.1	1.9 ± 0.3	6.7 ± 1.0
L20S	0.9 ± 0.1	0.6 ± 0.1	0.5 ± 0.1	0.4 ± 0.1	2.0 ± 0.3
L19K	0.5 ± 0.1	0.3 ± 0.1	0.3 ± 0.1	1.7 ± 0.2	3.8 ± 0.6
L20K	1.0 ± 0.1	0.7 ± 0.1	3.2 ± 0.3	4.4 ± 0.4	24.0 ± 4.5

[a] See Materials and Methods for experimental conditions and methods to calculate rate constants. Values of $(k_{cat}/K_m)_{app}$ represent mean values $\pm$ standard errors determined from a minimum of three measurements. [b] Triton X-100/sodium deoxycholate/diC_8PC (4:2:1) mixed micelles. [c] Polymerized mixed liposomes.

K_m, do not have well-defined implications. For this reason, we simply used an apparent second-order rate constant, $(k_{cat}/K_m)_{app}$, to compare activities of mutants under a given kinetic condition.

We first measured the activity of bovine pancreatic PLA_2 and mutants toward diC_6PC monomers. Although the microaggregation of enzyme and short-chain phospholipids below their critical micellar concentration has been observed for several secretory PLA_2s, the hydrolysis by pancreatic PLA_2s of diC_6PC below its critical micellar concentration (ca. 14 mM) follows the Michaelis−Menten kinetics and the degree of microaggregation is not significant, especially when the substrate concentration is low. Thus, the activity of bovine pancreatic PLA_2 (or its mutants) toward diC_6PC monomers (0.5 mM) largely depends on how productively the active site of the enzyme interacts with a monomer. For this study, we did not determine individual k_{cat} and K_m values with diC_6PC monomers because initial rate measurements necessary for these determinations require large amounts of proteins. Instead, we determined $(k_{cat}/K_m)_{app}$ from the reaction progress curves and summarized them in Table 2. All Leu-20 mutants showed activities toward monomeric diC_6PC comparable to that of wild type. In contrast, Leu-19 mutants displayed a wider range of activities. L19W was slightly more active than wild type, and the activity decreased with a decrease in hydrophobicity of the substituted side chain; the least active mutant, L19K, displayed ca. 50% of the wild-type activity. These results imply that Leu-19, but not Leu-20, be involved in the interaction with a monomeric substrate bound to the active site.

As described above, bovine pancreatic PLA_2 strongly prefers anionic interfaces to neutral ones due to its cationic interfacial binding residues. In order to accurately evaluate the contribution of hydrophobic residues of bovine pancreatic PLA_2 to its interfacial binding, it is therefore necessary to employ a phospholipid aggregate which has a neutral interface and yet is a good substrate for bovine PLA_2. For this purpose, we selected diC_8PC micelles which are good substrates for bovine pancreatic PLA_2 (see Table 2) due to their loose interfacial packing density. When assessed using these micellar substrates, the effects of Leu-19 mutations on the enzyme activity were similar to those observed with diC_6-PC monomers for L19W and L19S and more pronounced for L19K; L19W, L19S, and L19K showed 115%, 78%, and 15% of the wild-type activity, respectively. Conversely, the mutants of Leu-20 displayed completely different kinetic behaviors toward these diC_8PC micelles. L20S and L20K mutants showed only 30% and 35% of the wild-type activity, respectively, whereas L20W was ca. twice as active as wild type. In view of the above finding that all the Leu-20 mutants showed activities comparable to that of wild type toward the diC_6PC monomer, these data indicate that the mutations of Leu-20 change the interfacial binding affinity of bovine pancreatic PLA_2, which in turn points to the importance of Leu-20 in the hydrophobic interactions between the bovine pancreatic enzyme and micellar interfaces. To further investigate the effects of mutations on the interfacial catalysis of bovine PLA_2, we measured the activities of wild type and mutants toward PC molecules dispersed in Triton X-100/sodium deoxycholate/diC_8PC (4:2:1) mixed micelles. We previously showed (Dua & Cho, 1994) that these *anionic* mixed micelles are a good substrate for bovine pancreatic PLA_2. Toward these mixed micelles, the effects of the mutations on the enzyme activity were, in general, similar to those observed with diC_8PC micelles. L19W, L19S, and L19K retained 113%, 60%, and 19% of the wild-type activity, respectively, while L20W and L20S possessed 260% and 30% of the wild-type activity, respectively. Most interestingly, however, L20K which showed only 35% of the wild-type activity toward neutral diC_8PC micelles was twice as active as wild type toward anionic mixed micelles. This result shows that toward anionic interfaces the loss of hydrophobic interfacial binding could be compensated for by the gain of electrostatic interactions which, in turn, corroborates the notion that the residue in position 20 makes a direct contact with the surface of phospholipid aggregates.

Kinetic Properties of Mutants toward Polymerized Mixed Liposomes. Polymerized mixed liposomes serve as a useful kinetic system for PLA_2 in which phospholipids interacting with the active site of PLA_2 (i.e., hydrolyzable insert) are unambiguously distinguished from ones interacting with the interfacial binding site (i.e., polymerized matrix). In particular, this kinetic system allows one to determine the true substrate specificity of a PLA_2 because the variation of the head group or acyl chains of an inserted phospholipid, the composition of which is normally less than 5 mol %, does not significantly change the physical state of polymerized liposomes. Using polymerized mixed liposomes, we previously showed (Wu & Cho, 1993; Dua et al., 1995) that bovine PLA_2 preferred anionic pyrene-PG to zwitterionic pyrene-PC due to the presence of cationic active site groups. In general, secretory PLA_2s show no pronounced *sn*-2 acyl group selectivity among natural phospholipids because they bind in the hydrophobic channel only the first nine to ten carbons of the *sn*-2 acyl chain (Dennis, 1994). They can, however, distinguish synthetic phospholipids with shorter acyl chains (e.g., six to twelve carbons) and show definite *sn*-2 acyl group selectivity among them. Because the kinetic

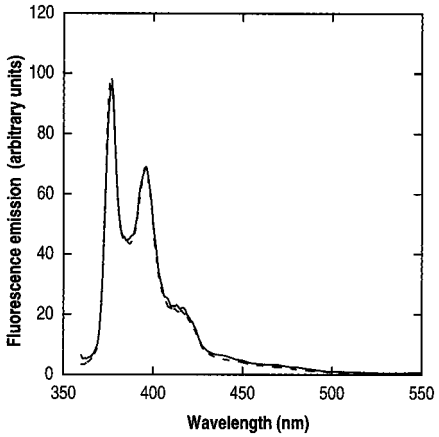

FIGURE 4: Fluorescence emission spectra of pyr-C_6PC/BLPG (solid line) and pyr-C_{12}PC/BLPG (broken line) polymerized mixed liposomes. Each solution contained 0.1 μM pyrene-containing PC inserted in 9.9 μM BLPG, 0.16 M NaCl, and 10 mM $CaCl_2$ in 10 mM HEPES buffer, pH 7.4. The excitation wavelength was set at 345 nm, and the spectral bandwidth was set at 5 nm for both excitation and emission.

data using monomers and micelles indicate that Leu-19 interacts with an active site bound substrate, we explored a possibility that Leu-19 is involved in the *sn*-2 acyl group selectivity by measuring the activities of wild type and mutants toward polymerized mixed liposomes containing hydrolyzable PC molecules with different *sn*-2 acyl groups. We did not measure the *sn*-1 acyl group selectivity because the *sn*-1 acyl group is not essential for the PLA_2−substrate interactions (Plesniak et al., 1995; Thunnison et al., 1990). Specifically, we used as an insert pyr-C_6PC and pyr-C_{12}PC which have hexyl and dodecanoyl groups in the *sn*-2 position, respectively. The structure of the common *sn*-1 acyl group, 12-(1-pyrenebutanoyloxy)dodecanoyl, was designed to resemble that of BLPG in order to optimize the miscibility of the polymerizable host and hydrolyzable inserts. We previously showed that 5 mol % of pyrene-PC molecules were uniformly distributed without forming patches over the surface of pyrene-PC/BLPG-polymerized mixed liposomes. To ensure that pyr-C_6PC and pyr-C_{12}PC are homogeneously dispersed in the polymerized matrix, we first measured the fluorescence spectra of pyr-C_6PC/BLPG (1:99 in mole ratio) and pyr-C_{12}PC/BLPG (1:99) polymerized mixed liposomes, respectively. As shown in Figure 4, no excimer peak of pyrene-containing PC was observed for both polymerized mixed liposomes, demonstrating the homogeneous distribution of inserts in the polymerized matrix of BLPG.

We then measured the activity of bovine pancreatic PLA_2 and mutants toward these polymerized mixed liposomes. As shown in Table 2, both pyr-C_6PC/BLPG- and pyr-C_{12}PC/BLPG-polymerized mixed liposomes were relatively poor substrates for bovine PLA_2 when compared to other substrates. Toward pyr-C_6PC/BLPG-polymerized mixed liposomes, L19W, L19S, and L19K retained 108%, 83%, and 74% of the wild-type activity, respectively. These effects were similar to those observed with diC_6PC monomer, although to a slightly lesser degree. In contrast, the effects of Leu-20 mutations were more pronounced than observed with diC_8PC micelles or with Triton X-100/sodium deoxycholate/diC_8PC mixed micelles. For instance, L20W was ca. six times more active than wild type whereas L20S had only 17% of the wild-type activity. Polymerized mixed liposomes are different from (mixed) micelles in that their interfaces are much more densely packed. Thus, the pronounced effects of these mutations observed with polymerized mixed liposomes indicate that Trp at position 20 enhanced the binding of PLA_2 to densely packed interfaces, which was reduced significantly with Ser. Furthermore, the finding that L20K showed the same 2-fold increase in activity toward anionic mixed micelles and toward anionic polymerized mixed liposomes again indicates that its activation derived from enhanced electrostatic interactions between Lys-20 and anionic interfaces. The activity of bovine pancreatic PLA_2 toward pyr-C_{12}PC/BLPG-polymerized mixed liposomes was ca. five times higher than that toward pyr-C_6PC/BLPG-polymerized mixed liposomes, which represents the true *sn*-2 acyl group selectivity of bovine pancreatic PLA_2. In agreement with the above kinetic data, all Leu-20 mutants showed essentially the same *sn*-2 acyl group selectivity. Also, L19W showed the similar selectivity. Conversely, L19K showed significantly reduced acyl group selectivity, hydrolyzing pyr-C_{12}PC only twice faster than pyr-C_6PC in polymerized mixed liposomes, and L19S was 3.5 times more active toward pyr-C_{12}PC than toward pyr-C_6PC. These results indicate that Leu-19 is involved in the *sn*-2 acyl group selectivity of bovine pancreatic PLA_2.

Table 3: Binding of Bovine Pancreatic PLA_2 and Its Mutants to the D-diC_6PC Monomer and BLPG-Polymerized Liposome[a]

	D-diC_6PC monomer	BLPG polymerized liposome	
enzyme	K_d (mM)	n	K_d (nM)
wild type	2.0 ± 0.3	30 ± 5	40 ± 5
L19W	2.0 ± 0.3	nd	nd
L20W	2.1 ± 0.3	28 ± 6	8 ± 1
L19K	3.0 ± 0.2	32 ± 5	42 ± 5
L20K	2.1 ± 0.2	31 ± 4	22 ± 4

[a] See Materials and Methods for experimental conditions and methods to calculate dissociation constants. Values of n and K_d represent best values ± standard deviations determined from the nonlinear least-squares analysis. [b] nd, not determined.

Binding of Mutants to Monomers, Polymerized Liposomes, and Monolayers. In order to determine the origin of altered kinetic behaviors of bovine PLA_2 mutants, we measured their binding to various phospholipids. We first spectrophotometrically measured the binding of proteins to a nonhydrolyzable D-diC_6PC monomer. It was shown that short-chain D-phospholipids, although not conducive to PLA_2 catalysis, bound to the active site of the enzyme as well as the L-isomers did (Pieterson et al., 1974). The K_d values of bovine PLA_2 and selected mutants determined from their binding isotherms (data not shown) are summarized in Table 3. In agreement with kinetic data, the mutations of Leu-20, e.g., L20W and L20K, did not have a significant effect on the monomer binding. Also, L19W showed no significant change in monomer binding whereas the L19K mutation resulted in a 50% decrease in monomer binding. These results indicate that Leu-19, but not Leu-20, interacts with active-site-bound substrate and its substitution with an ionic residue considerably disrupts the binding.

We previously showed that the inertness of BLPG-polymerized liposomes to PLA_2 hydrolysis allows one to directly determine thermodynamic parameters for the binding of PLA_2 to pyrene-PC/BLPG-polymerized mixed liposomes. We determined the dissociation constant for a PLA_2-polymerized liposome complex for bovine PLA_2 and selected mutants. The binding isotherms of bovine PLA_2 and mutants

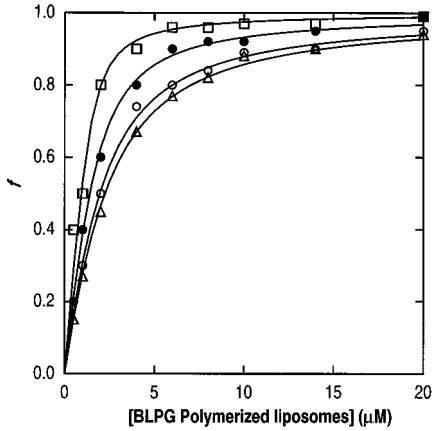

FIGURE 5: Binding isotherms of bovine pancreatic PLA_2 (○) and its mutants including L20W (□), L20K (●), and L19K (△). Protein concentrations were 50 nM. See Materials and Methods for the definition of *f*. The solid lines indicate theoretical curves constructed using eq 1 with *n* and K_d values determined from nonlinear least-squares analyses.

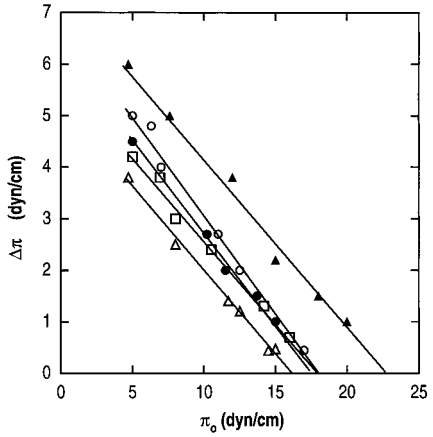

FIGURE 6: Effect of initial surface pressure (π_0) of the D-POPC monolayer on the penetration ($\Delta\pi$) of bovine pancreatic PLA_2 (○) and its mutants including L19W (□), L20W (▲), L19K (●), and L20K (△). The protein concentration in the subphase was 0.15 μM. Each solid line indicates the extrapolation of the $\Delta\pi$ vs π_0 plot to the abscissa axis.

to BLPG-polymerized liposomes are shown in Figure 5 and thermodynamic parameters determined from the data analysis are summarized in Table 3. As described under Materials and Methods, our previous fluorometric method, although experimentally convenient, entailed the use of high protein concentration (ca 2 μM) and thus was not ideal for the accurate determination of the dissociation constants for the mutants with enhanced interfacial binding affinity (e.g., K_d = 8 nM for L20W). For this reason, *n* and K_d values for selected mutants were determined from the centrifugation method using sucrose-loaded polymerized liposomes which allowed a more accurate determination of these values. Sucrose-loaded BLPG-polymerized liposomes were essentially indistinguishable from BLPG-polymerized liposomes. For instance, light scattering measurements indicated that both polymerized liposomes had the same size (100 ± 10 nm). Also, bovine pancreatic PLA_2 showed the same activity toward pyrene-PC/BLPG-polymerized mixed liposomes and sucrose-loaded pyrene-PC/BLPG-polymerized mixed liposomes (B.-I. Lee and W. Cho, unpublished observation). Finally, *n* and K_d values for bovine pancreatic PLA_2 determined using sucrose-loaded BLPG-polymerized liposomes were identical to those determined using BLPG-polymerized liposomes (Dua et al., 1995).

As shown in Figure 5, the binding isotherms of bovine PLA_2 and mutants showed an identical hyperbolic pattern, indicating the lack of unusual binding mode caused by mutations, and all the proteins had essentially the same *n* values (ca. 30). In reasonable agreement with their relative kinetic activity toward pyr-C_6PC (or pyr-C_{12}PC)/BLPG-polymerized mixed liposomes, L20W and L20K showed a 5-fold and a 2-fold decrease in K_d value when compared to wild type, again indicating that enhanced activity of these mutants toward polymerized mixed liposomes was mainly due to an increase in their interfacial binding. Interestingly, L19K possessing only 20% of the wild-type activity toward pyr-C_6PC (or pyr-C_{12}PC)/BLPG-polymerized mixed liposomes had nearly the same K_d value as wild type, demonstrating that L19K mutation did not affect the interfacial binding *per se*.

To further support the notion that Leu-19 is involved in the substrate binding and Leu-20 in the interfacial binding, we measured the interactions of bovine PLA_2 and selected mutants with phospholipid monolayers at the air−water interface. Phospholipid monolayers are an excellent model membrane in which the interfacial packing density of phospholipid can be readily and precisely varied and the penetration of protein into phospholipids can be sensitively monitored in terms of the change in surface pressure ($\Delta\pi$) (Verger & Pattus, 1982). It was previously reported (Demel et al., 1975) that pancreatic PLA_2s could not readily hydrolyze densely packed zwitterionic PC monolayers and bilayers because of their weak penetrating power. If Leu-20 of bovine PLA_2 is indeed involved in the interfacial binding, this hydrophobic side chain would penetrate, at least partially, into the hydrophobic core of phospholipid monolayers (or bilayers). In contrast, Leu-19 is not expected to penetrate into phospholipid monolayers and achieve this hydrophobic interfacial binding. Thus, the substitution of Leu-20 with a polar residue would have a significant effect on the monolayer penetration of bovine PLA_2 whereas the mutation of Leu-19 would not. To explore this possibility, we measured the penetration of bovine pancreatic PLA_2 and selected mutants into the nonhydrolyzable D-POPC monolayer as a function of its initial surface pressure (π_0); a higher π_0 value indicates higher phospholipid packing density. As shown in Figure 6, the penetration of bovine pancreatic PLA_2 measured in terms of $\Delta\pi$ showed a monotonous decrease with the increase in π_0, which is typical for the binding of surface-active proteins to monolayers. The degree of its penetration was, however, much smaller than that caused by other surface-active proteins, which normally reaches up to 15 dyn/cm (Verger & Pattus, 1982). Also, bovine PLA_2 was unable to penetrate into the D-POPC monolayer when $\pi_0 > 20$ dyn/cm. Finally, Ca^{2+} did not have any detectable effect on the penetration behaviors of proteins, indicating that the observed penetration was not due to the substrate binding. Evidently, bovine PLA_2 has low membrane-penetrating capacity and cannot penetrate into biological membranes whose estimated surface pressure is ca. 31 dyn/cm. Given that, the effects of mutations on the monolayer penetration of bovine PLA_2 were well consistent with kinetic and binding data. Both L19K and L19W showed the monolayer binding behaviors which were not significantly different from that of wild type, indicating that Leu-19 was not directly involved in the monolayer penetration. Con-

versely, Leu-20 mutants displayed distinct monolayer binding behaviors. On one hand, L20W showed higher $\Delta\pi$ values than wild type at the measured π_0 range and was able to penetrate the monolayer with π_0 up to 25 dyn/cm. On the other hand, L20K showed lower $\Delta\pi$ values than wild type at the measured π_0 range and showed no detectable penetration when $\pi_0 > 16$ dyn/cm, Taken together, these results support the notion that Leu-20 is involved in hydrophobic interfacial binding and Leu-19 is in substrate binding. Furthermore, they showed that the substitution of Leu-20 with amphiphilic Trp considerably improved the monolayer penetration and interfacial binding which was greatly disrupted by the substitution with an ionic residue.

DISCUSSION

Secretory PLA_2s are one of the most thoroughly characterized enzymes in terms of protein structure; high-resolution X-ray crystallographic structures are available for more than ten natural and recombinant species. Yet, the exact mechanism of interfacial binding and the identity of interfacial binding residues are relatively poorly understood due to the lack of explicit structural information on the membrane-bound PLA_2. Among surface hydrophobic residues forming the rim of the hydrophobic channel, at least two residues, i.e., Trp-3 and Leu-20, have a side-chain orientation distinct from the rest of group (see Figure 1). Specifically, their side chains are oriented perpendicular to the entrance of hydrophobic channel whereas the side chains of other hydrophobic residues, including Leu-19, point to the entrance of the hydrophobic channel. The involvement of Trp-3 in the interfacial binding of bovine pancreatic PLA_2 has been well documented (Jain & Maliwal, 1993; Liu et al., 1995; Maliwal et al., 1994). The present study not only demonstrates the importance of Leu-20 in the interfacial binding of the bovine enzyme but also reveals the involvement of its neighboring Leu-19 in the substrate binding and *sn*-2-acyl group selectivity. As expected from their surface locations, our CD and chemical denaturation data of mutants showed that the substitutions of Leu-19 and Leu-20 with serine, lysine, and tryptophan, respectively, did not significantly change either the tertiary structure or the thermodynamic stability of bovine pancreatic PLA_2. These results, therefore, precluded a possibility that the observed kinetic and binding behaviors of mutants resulted from any major deleterious structural changes. Rigorously speaking, the changes in rate constant by the mutations should be regarded as upper limit values because local conformational changes by the mutations were not determined. We suspect that, however, only minor local structural changes resulted from the mutations at these two positions for several reasons. First, serine and, more frequently, tryptophan residues are found in these positions for other PLA_2s. Second, a recent mutagenesis study (Liu et al., 1995) showed that mutations of residues forming the rim of the hydrophobic channel of bovine pancreatic PLA_2 did not significantly change the local conformation whereas mutations of residues inside the hydrophobic channel (e.g., Phe-5, Ile-9) resulted in drastic structural and kinetic changes. Finally, our kinetic and binding data clearly showed that no mutants drastically lost their functions; they fully retained either the interfacial binding affinity or the substrate binding affinity.

Roles of Leu-19. Kinetic and binding properties of Leu-19 mutants show that Leu-19 is involved in substrate binding but not in interfacial binding . A previous mutational study on Leu-31 of porcine pancreatic PLA_2 (Kuipers et al., 1990) showed that decreased activities of its mutants, including L31R and L31S which are similar to L19K and L19S described in the present report, were due to the k_{cat} effect rather than the K_m effect. On the basis of this observation, authors concluded that Leu-31 played a role of properly orienting an active-site-bound substrate. A similar effect was observed with the mutation of Leu-2 of bovine pancreatic PLA_2; e.g., L2R had a 500-fold reduction in k_{cat} and altered *sn*-2 acyl group selectivity (Liu et al., 1995). However, the effect on the *sn*-2 acyl group selectivity was not unambiguously demonstrated as it was estimated from the relative activity of wild type and mutant toward two phospholipid substrates that formed different types of aggregates, i.e., micelles and liposomes. For the reason described under Results, we did not separately determine k_{cat} and K_m for our kinetic studies but instead used an apparent second-order constant, $(k_{cat}/K_m)_{app}$, to describe the relative activity of mutants. Then, we compared this kinetic constant with the dissociation constant independently determined from binding measurements to sort out the effects of mutations on different enzymatic processes. Furthermore, we unambiguously determined the *sn*-2 acyl group selectivity of bovine pancreatic PLA_2 and mutants using our polymerized mixed liposomes. The kinetic data summarized in Table 2 show that effects of Leu-19 mutations are, in general, less drastic than observed for Leu-2 and Leu-31 mutations. With micellar substrates, the activity decrease for the L31S mutation of porcine pancreatic PLA_2 was up to 40-fold and the activity increase for the L31W mutation was ca. 3-fold. Under similar conditions, the L2R mutation of bovine pancreatic PLA_2 reduced the activity by 3 orders of magnitude. In the case of Leu-19 of bovine pancreatic PLA_2, the maximal activity decrease due to mutation was ca. 7-fold for L19K and the activity increase for the L19W mutation was only 15%. Furthermore, the kinetic and binding properties of Leu-19 mutants toward the diC_6PC monomer showed that the change in enzyme activity was even less and derived mainly from the K_m effect. Thus, it appears that although Leu-19 of bovine PLA_2 is involved in the substrate binding, it does not play a role of properly orienting the substrate in the active site. Also, its contributions to the substrate binding are not as important as those from Leu-2 and Leu-31. Indeed, the crystal structure of the porcine pancreatic PLA_2−inhibitor complex (Thunnison et al., 1990) shows that the side chains of Leu-2 and Leu-31 are closer to the *sn*-2 acyl chain of the inhibitor, 2-(dodecanoylamino)-1-hexanoylphosphoglycol, than that of Leu-19; e.g., the side chain C_γ of Leu-2 is 3.65 Å away from the C_{12} of the *sn*-2 acyl chain of the inhibitor whereas the minimal distance between Leu-19 and the inhibitor is 4.87 Å between the C_δ of Leu-19 and the C_8 of the *sn*-2 acyl chain of the inhibitor. A recent NMR structural analysis showed (Plesniak et al., 1995) that the conformation of the *sn*-2 acyl group of the inhibitor bound to the active site of *N. naja naja* PLA_2, which has a large Trp residue at the position 19, changed greatly as its length increased from six to nine. This structural information is well consistent with the findings that the L19K mutation had relatively small effects on the activity of bovine pancreatic PLA_2 toward diC_6-PC monomers and pyr-C_6PC/BLPG-polymerized mixed liposomes and much larger effects toward diC_8PC in micelles and pyr-C_{12}PC in polymerized mixed liposomes. Presum-

ably, the side chain of Lys-19 does not directly contact short acyl chains of active-site-bound diC_6PC and pyr-C_6PC but interacts unfavorably with longer acyl chains of diC_8PC and pyr-C_{12}PC. As a result, L19K showed significantly reduced *sn*-2 acyl group selectivity compared to wild type. Similarly, L19S with a smaller polar side chain at position 19 showed less *sn*-2 acyl group selectivity than wild type. Taken together, our results indicate that Leu-19 interacts with the *sn*-2 acyl group of an active-site-bound substrate, presumably the seventh to tenth carbon located near the entrance of the hydrophobic channel.

Roles of Leu-20. Position 20 of secretory PLA_2s is mostly occupied by hydrophobic residues, such as Leu, Ile, and Val, and by Trp for most cobra venom PLA_2s. Kinetic and binding properties of Leu-20 mutants demonstrate that Leu-20 is involved in the *hydrophobic* interfacial binding but not in substrate binding. None of the Leu-20 mutants showed altered activity toward monomeric diC_6PC and altered *sn*-2 acyl group selectivity. These mutations caused, however, significant changes in kinetic and binding properties of bovine pancreatic PLA_2 toward aggregated phospholipids, and the changes were sensitive to the interfacial properties of aggregates. The L20S mutation resulted in a 3-fold to 6-fold decrease in activity depending on the interfacial packing density. The changes were not sensitive to the surface charge of aggregates, as witnessed by similar rate decreases toward neutral micelles and toward anionic mixed micelles. In contrast, the effect of L20K mutation was highly dependent on the surface charge. As is the case with the L20S mutation, this mutation decreased the hydrophobic interfacial binding as shown by lower activity of L20K toward diC_8PC micelles and its weaker penetration into D-POPC monolayers. Toward anionic micelles and liposomes, however, the decrease was outweighed by the increase in electrostatic interactions. We previously showed (Shen et al., 1994), by chemically acylating with long-chain fatty acids two lysines critically involved in the interfacial binding of *A. piscivorus piscivorus* PLA_2, that a loss of electrostatic interfacial binding could be compensated for by a gain of hydrophobic interfacial binding. Thus, L20K provides an opposite example for the same theme that the interfacial binding of PLA_2 is driven by the combination of electrostatic and hydrophobic interactions, the relative importance of which depends on the interfacial properties of phospholipid aggregates. Assuming that a ca. 3-fold decrease in activity toward diC_8PC micelles caused by the L20S or L20K mutation was entirely due to the decrease in interfacial binding, one can estimate an upper limit of the contribution of Leu-20 to hydrophobic interfacial binding using an equation: $\Delta\Delta G^\circ = -RT \ln 3 = 0.65$ kcal/mol at room temperature (Fersht, 1985). This estimated value is close to the contribution from one methylene unit to hydrophobic interactions and, thus, suggests that Leu-20 might penetrate only partially into the phospholipid monolayer. Indeed, this notion is consistent with the monolayer penetration behaviors of bovine pancreatic PLA_2 and mutants. Bovine PLA_2 displayed relatively low monolayer penetration, which was slightly decreased by the L20K mutation but considerably increased by the L20W mutation. The amphiphilic indole side chain of tryptophan has been shown to partition at the lipid−water interface in lipid bilayers (Jacobs & White, 1989). Also, tryptophans are frequently found at the lipid−water interface and play an important role in membrane−protein interactions for many membrane proteins, including gramicidin A in which the indole N−H group forms a hydrogen bond with acyl carbonyl oxygens (Hu et al., 1993). Presumably, Trp-20 outperformed leucine in terms of the binding to the D-POPC monolayer and BLPG-polymerized liposomes because Leu-20 of bovine pancreatic PLA_2 does not penetrate deeply into the hydrophobic core of the monolayer and because tryptophan is intrinsically more efficient than leucine at the lipid−water interface. Because it is difficult to directly measure the concentration of protein bound to the phospholipid monolayer, it is not clear from the monolayer data whether a larger $\Delta\pi$ value for L20W at a given π_0 indicates higher surface concentration of protein or simply reflects the size of the indole ring which occupies a larger surface area than the side chain of leucine (or both). Enhanced binding affinity of L20W to BLPG-polymerized liposomes, however, supports the notion that the tryptophan increases the concentration of surface-bound protein. Also, the unique amphiphilic mode of the action of tryptophan at the lipid−water interface might allow it to bind more efficiently than hydrophobic side chains to densely packed interfaces that would not allow the penetration of hydrophobic side chains of proteins. Many cobra venom PLA_2s with high intrinsic activity toward densely packed PC bilayers, most notably *N. naja naja* PLA_2, contain the tryptophans at positions 19 and 20. Kinetic and binding properties of L20W presented herein demonstrate the importance of Trp-20 in the actions of these venom PLA_2s. In an attempt to enhance the interfacial activity of porcine pancreatic PLA_2 by simulating the structure of *N. naja naja* PLA_2, Kuiper et al. (1989) deleted the so-called elapid loop which spans residues 62−66 and is unique to class I pancreatic PLA_2s. Although the resulting mutant was up to 16 times more active than wild type toward PC micelles, the rate enhancement was mainly due to the improved substrate binding because the same mutant showed a 4-fold rate decrease toward anionic micelles. In contrast, L20W showed the same rate increase toward pyrene-PC/BLPG- and pyrene-PG/BLPG-polymerized mixed liposomes (B.-I. Lee and W. Cho, unpublished observation). To demonstrate that L20W has truly higher interfacial binding affinity than wild type, we measured the activity of bovine pancreatic PLA_2, L20K, and L20W toward densely packed neutral bilayers,

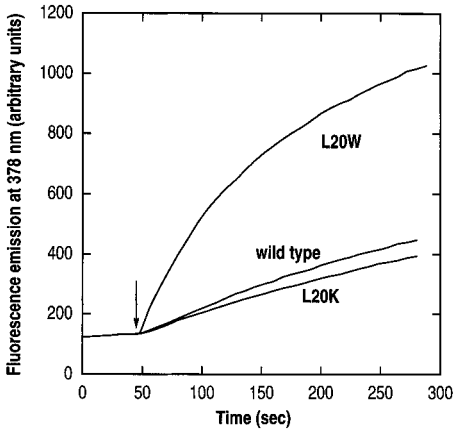

FIGURE 7: Kinetic courses of the hydrolysis of pyrene-PC/BLPC polymerized mixed liposomes by bovine pancreatic PLA_2, L20W, and L20K at 37 °C and at pH 7.4. Reaction mixtures contain 0.5 μM pyrene-PC, 9.5 μM BLPC, 5 μM BSA, 0.16 M NaCl, 10 mM $CaCl_2$, and 2 μM enzyme. The arrow indicates the addition of enzyme to the mixture.

pyrene-PC/BLPC-polymerized mixed liposomes. As shown in Figure 7, these polymerized liposomes were a extremely poor substrate for bovine pancreatic PLA_2 and L20K. However, L20W was able to hydrolyze these bilayers much more efficiently than wild type. The increase in activity estimated from the relative initial rate was ca. 7-fold. Thus, L20W represents the first example of protein engineering of PLA_2 which results in a significant increase in the interfacial binding to densely packed neutral monolayers and bilayers. Further mutagenesis studies are under way to fully understand the molecular origin of different activities of bovine pancreatic PLA_2 and *N. naja naja* PLA_2 that can readily hydrolyze PC monolayers and bilayers with π_0 up to 35 dyn/cm.

REFERENCES

Budzynski, D. M., Benight, A. S., LaBrake, C. C., & Fung, L. W.-M. (1992) *Biochemistry 31*, 3653−3660.

Demel, R. A., Geurts van Kessel, W. S. M., Zwaal, R. F. A., Roelofsen, B., & van Deenen, L. L. M. (1975) *Biochim. Biophys. Acta 406*, 97−107.

Deng, T., Noel, J. P., & Tsai, M.-D. (1990) *Gene 93*, 229−234.

Dennis, E. A. (1994) *J. Biol. Chem. 269*, 13057−13060.

Dijkstra, B. W., Drenth, J., & Kalk, K. H. (1981a) *Nature 289*, 604−606.

Dijkstra, B. W., Kalk, K. H., Hol, W. G. J., & Drenth, J. (1981b) *J. Mol. Biol. 147*, 97−123.

Dua, R., & Cho, W. (1994) *Eur. J. Biochem. 221*, 481−490.

Dua, R., Wu, S.-K., & Cho, W. (1995) *J. Biol. Chem. 270*, 263−268.

Fersht, A. (1985) *Enzyme Structure and Mechanism*, W. H. Freeman and Co., New York.

Gelb, M. H., Jain, M. K., Hanel, A. M., & Berg, O. G. (1995) *Annu. Rev. Biochem. 64*, 653−688.

Hu, W., Lee, K.-C., & Cross, T. A. (1993) *Biochemistry 32*, 7035−7047.

Jacobs, R. E., & White, S. H. (1989) *Biochemistry 28*, 3421−3437.

Jain, M. K., & Berg, O. G. (1989) *Biochim. Biophys. Acta 1002*, 127−156.

Jain, M. K., & Maliwal, B. P. (1993) *Biochemistry 32*, 11838−11846.

Kates, M. (1986) *Techniques of Lipidology*, 2nd ed., Elsevier, Amsterdam.

Kini, R. M., & Evans, H. J. (1987) *J. Biol. Chem. 262*, 14402−14407.

Kuipers, O. P., Dijkman, R., Cornelieke, E. G. M. P., Verheij, H. M., & De Haas, G. H. (1989) *Protein Eng. 2*, 467−471.

Kuipers, O. P., Kerver, J., van Meersbergen, J., Vis, R., Dijkman, R., Verheij, H. M., & De Haas, G. H. (1990) *Protein Eng. 3*, 599−603.

Liu, X., Zhu, H., Huang, B., Rogers, J., Yu, B.-Z., Kumar, A., Jain, M. K., Sundaralingam, M., & Tsai, M.-D. (1995) *Biochemistry 34*, 7322−7334.

Maliwal, B. P., Yu, B.-Z., Szmacinski, H., Squier, T., van Binsbergen, J., Slotboom, A. J., & Jain, M. K. (1994) *Biochemistry 33*, 4509−4516.

Mukhopadhyay, S., & Cho, W. (1995) *Biochim. Biophys. Acta* (in press).

Nakamaye, K., & Eckstein, F. (1986) *Nucleic Acids Res. 14*, 9679−9698.

Pace, C. N. (1986) *Methods Enzymol. 131*, 266−280.

Pieterson, W. A., Vidal, J. C., Volwerk, J. J., & de Haas, G. H. (1974) *Biochemistry 13*, 1455−1460.

Plesniak, L. A., Yu, L., & Dennis, E. A. (1995) *Biochemistry 34*, 4943−4951.

Rebecchi, M., Peterson, A., & McLaughlin, S. (1992) *Biochemistry 31*, 12742−12747.

Santoro, M. M., & Bolen, D. W. (1988) *Biochemistry 27*, 8063−8068.

Scott, D. L., & Sigler, P. B. (1994) *Adv. Protein Chem. 45*, 53−88.

Scott, D. L., White, S. P., Otwinowski, Z., Gelb, M. H., & Sigler, P. B. (1990) *Science 250*, 1541−1546.

Shen, Z., & Cho, W. (1995) *Int. J. Biochem. Cell Biol. 27*, 1009−1013.

Shen, Z., Wu, S.-K., & Cho, W. (1994) *Biochemistry 33*, 11598−11607.

Smith, P. K., Krohn, R. I., Hermanson, G. T., Mallia, A. K., Gartner, F. H., Provenzano, M. D., Fujimoto, E. K., Goeke, N. M., Olson, B. J., & Klenk, D. C. (1985) *Anal. Biochem. 150*, 76−85.

Thunnison, M. M. G. M., AB, E., Kalk, K. H., Drenth, J., Dijkstra, B. W., Kuiper, O. P., Dijkman, R., de Haas, G. H., & Verheij, H. M. (1990) *Nature 347*, 689−691.

Verger, R., & Pattus, F. (1982) *Chem. Phys. Lipids 30*, 189−227.

Woody, R. W. (1994) in *Circular Dichroism Principles ans Applications* (Nakanish, K., Berova, N., & Woody, R. W., Eds.) pp 473−496, VCH Publishers, New York, NY.

Wu, S.-K., & Cho, W. (1993) *Biochemistry 32*, 13902−13908.

Wu, S.-K., & Cho, W. (1994) *Anal. Biochem. 221*, 152−159.

BI9524777